Available online at www.sciencedirect.com
SCIENCE DIRECT®
PERGAMON
Polyhedron 22 (2003) 1213–1219
POLYHEDRON
www.elsevier.com/locate/poly

Studies on the zinc(II)-azoimine system. Single-crystal X-ray structure of $Zn(MeaaiMe)Cl_2 \cdot H_2O$ and $Zn(HaaiMe)_2(NCS)_2$ (MeaaiMe = 1-methyl-2-(*p*-tolylazo)imidazole, HaaiMe = 1-methyl-2-(phenylazo) imidazole)

B.G. Chand [a], U.S. Ray [a], J. Cheng [b], T.-H. Lu [b], C. Sinha [a,*]

[a] *Department of Chemistry, The University of Burdwan, Burdwan 713104, India*
[b] *Department of Physics, National Tsing Hua University, Hsinchu 300, Taiwan, ROC*

Received 15 May 2002; accepted 21 January 2003

Abstract

Dichloro zinc(II) complexes of 1-alkyl-2-(arylazo)imidazole, $Zn(RaaiR')Cl_2 \cdot H_2O$ (RaaiR′ = *p*-R–C_6H_4–N = N–C_3H_2N–N(1)–R′: R = H, Me, Cl and R′ = Me, CH_2CH_3, CH_2Ph) are characterized by elemental analysis, IR, UV–Vis and ^1H NMR spectral data. The reaction of $ZnCl_2$ and RaaiR′ (excess) in the presence of NH_4CNS has synthesized $Zn(RaaiR')_2(NCS)_2$. The single-crystal X-ray structure of dichloro-{1-methyl-2-(*p*-tolylazo)imidazole}zinc(II)-monohydrate ($Zn(MeaaiMe)Cl_2 \cdot H_2O$) suggests that the complex is distorted trigonal bipyramidal (TBP) around Zn(II) with a trigonal plane constituted from Cl(1), Cl(2), *N*(imidazole) (N(1)). Molecular packing shows a 1D chain via a hydrogen bonded eight membered ring. The X-ray structure of di-thiocyanato-bis-{1-methyl-2-(phenylazo)-imidazole}zinc(II) also shows a distorted TBP around Zn(II). The coordination sphere is ZnN_3 type: where one of the ligands acts as a bidentate chelating agent and the second one coordinates via only the imidazole-N along with two N-centers from the NCS group.
© 2003 Elsevier Science Ltd. All rights reserved.

Keywords: Arylazoimidazole; Zinc(II) complexes; Crystal structures; Hydrogen bonding; 1D chain

1. Introduction

Zinc complexes with heterocyclic N-donor ligands offer a potential agent to mimic different zinc containing metalloproteins. For example, the active site coordination geometry of liver alcohol dehydrogenase is a mononuclear zinc center ligated in a tetrahedral array by two histidine nitrogen, two cystine thiolates and a water molecule [1], super oxide dismutase binds Cu(II) and Zn(II) via an imidazolate bridge [2,3], etc. The specific role played by the imidazole active center of a large number of metalloproteins has encouraged the design of many imidazole containing ligands from view points of coordination chemistry [4,5]. Although zinc is redox inactive in most cases it provides the structural integrity to the polymetallo-enzymes so that the redox active metal ion may exhibit maximum efficiency. The active site is connected to a network of hydrogen bonds formed by adjacent residues and water molecules. It has been demonstrated that $L_3Zn–OH_2$ (L = coordinated parts of enzyme) is the active species in the dehydration of HCO_3^- in carbonic anhydrase [6,7]. Design of model zinc(II) complexes having labile H_2O coordination is a real challenge [8].

In an effort towards the design of imidazole containing ligands we have synthesized arylazoimidazoles [9–11]. The molecule is π-acidic and the active function is the azoimine group (–N=N–C=N–). They have been used successfully to stabilize lower metal oxidation states viz. Cu(I), Ru(II), Os(II). We have intensively developed the coordination chemistry [9–11] and analytical application of arylazoimidazoles [12,13]. Major developments have been carried out in the field of

* Corresponding author. Tel.: +91-342-557683; fax: +91-342-530452.
E-mail address: c_r_sinha@yahoo.com (C. Sinha).

0277-5387/03/$ - see front matter © 2003 Elsevier Science Ltd. All rights reserved.
doi:10.1016/S0277-5387(03)00111-6

transitions metals [9–11]. The non-transition metal chemistry of this function is scarce [14–16]. The coordination chemistry of zinc with 1-alkyl-2-(arylazo)-imidazole has remained unexplored. In this article, we report the synthesis, spectral properties, chemical reactivity of zinc(II) complexes of 1-alkyl-2-(arylazo)imidazole. The single-crystal X-ray structure of one of the complexes has shown a hydrogen bonded 1D chain via coordinated water. The synthesis and X-ray structure of the thiocyanato derivative are also reported here.

2. Experimental

2.1. Materials

1-Alkyl-2-(arylazo)imidazoles were prepared by the reported procedure [9]. [*n*-Bu_4N][ClO_4] and MeCN for electrochemical work were purified by an earlier procedure [10]. All other chemicals and solvents were of reagent grade and used as received.

2.2. Physical measurements

Details of physical measurements are described in Ref. [14].

2.3. Synthesis of [Zn(MeaaiMe)Cl_2·H_2O] (**4b**)

1-Methyl-2-(*p*-tolylazo)imidazole (0.1 g, 0.5 mmol) in MeOH (10 cm^3) was added dropwise to a stirred methanolic solution (10 cm^3) of $ZnCl_2$ H_2O (0.077 g, 0.5 mmol) at room temperature over a period of 3 h. The volume of the orange–red solution was reduced to half of its original volume by slow evaporation in air. The solution was then kept in a refrigerator maintaining the temperature at 5 °C. The bright orange–red crystalline product was then precipitated out. The product was filtered, washed with water and cold MeOH. The product was then recrystallised from MeOH–H_2O (1:1, v/v) and dried over $CaCl_2$. The yield was 0.124 g, 70%.

All other zinc complexes were prepared similarly and the yield varied from 40 to 60%. The microanalytical data of the complexes are given in Table 2. Zinc was estimated by complexometric titration [17].

2.4. Synthesis of Zn(HaaiMe)$_2$(NCS)$_2$ (**7a**)

A methanol solution (15 cm^3) of MeaaiMe (0.186 g, 1 mmol) was added to a stirred solution of $ZnCl_2$·H_2O (0.077 g, 0.5 mmol) and NH_4CNS (0.076 g, 1 mmol) at room temperature The stirring was continued for 1 h and then the orange–yellow solution was filtered. The solution was evaporated slowly in air and an orange crystalline product deposited on the wall of the beaker. It was collected and dried over $CaCl_2$.The yield was 0.1892 g, 65%.

All other zinc complexes were prepared similarly and the yield varied from 40 to 60%. The microanalytical data of the complexes are given in Table 2.

Table 1
Crystallographic data

	Zn(MeaaiMe)Cl_2·H_2O (**4b**)	Zn(HaaiMe)$_2$(NCS)$_2$ (**7a**)
Empirical formula	$C_{11}H_{14}Cl_2N_4OZn$	$C_{22}H_{20}N_{10}S_2Zn$
Formula weight	354.53	553.97
Temperature (K)	293 (2)	294
Crystal system	monoclinic	monoclinic
Space group	$P2_1/c$	$P2_1/c$
Crystal size (mm)	0.30 × 0.30 × 0.30	0.30 × 0.30 × 0.40
Unit cell dimensions		
a (Å)	7.878(2)	8.9562(8)
b (Å)	11.0625(14)	15.3366(13)
c (Å)	17.011(7)	19.2868(17)
α (°)	90	90
β (°)	98.69(3)	92.647(2)
γ (°)	90	90
V(Å^3)	1465.4(8)	2646.4(4)
Z	4	4
2θ-range (°)	4–56	4–56
λ (Å)	0.71073	0.71073
μ (Mo Kα)	2.037	1.116
D_{calc} (Mg m^{-3})	1.607	1.390
Refined parameters	181	316
R_1^a [$I > 2\sigma$ (I)]	0.0250	0.0462
wR_2^b	0.0723	0.1276
Goodness of fit	1.090	0.930

2.5. X-ray diffraction study

Crystal parameters and refinement results are summarized in Table 1. For Zn(MeaaiMe)Cl_2·H_2O (**4b**) diffraction data were collected from an Enraf-Nonius CAD-4 diffractometer using graphite monochromatised Mo Kα radiation ($\lambda = 0.71073$ Å). Data collections were performed in the 2θ range 4–56°. For Zn(HaaiMe)$_2$(NCS)$_2$ (**7a**) the data were collected by a SMART CCD diffractometer at 293(2) K using graphite monochromatized Mo Kα radiation. Data collections were performed in the 2θ range 3 to 56°. The data were corrected for linear decay as three reference reflections were monitored throughout the data collection. Empirical absorption corrections were carried out based on ω-scans. The structure was solved by the heavy atom method and refined by full-matrix least-squares refinement based on F_o^2 and including all reflections. All non-hydrogen atoms were refined anisotropically. Hydrogen atoms bonded to aromatic carbons were included at

Table 2
Microanalytical [a], UV–Vis [b] and voltammetric data [c]

Compounds	Microanalytical data			UV–Vis spectral data	Ligand reduction
	Found (calc.)%			λ_{max} (nm) (10^{-3} ε ($dm^3\,mol^{-1}\,cm^{-1}$))	V
	C	H	N		
$Zn(HaaiMe)Cl_2\cdot H_2O$ (**4a**)	35.15(35.25)	3.4(3.52)	16.48(16.45)	435(7.37), 378(17.62), 278(3.93), 232(9.06)	−0.48, −1.22
$Zn(MeaaiMe)Cl_2\cdot H_2O$ (**4b**)	37.14(37.24)	3.85(3.95)	15.93(15.80)	444(7.18), 383(17.62), 275(5.95), 244(7.08)	−0.50, −1.38
$Zn(ClaaiMe)Cl_2\cdot H_2O$ (**4c**)	31.91(32.01)	2.83(2.93)	14.97(14.93)	440(6.92), 380(18.20), 278(6.18), 240(7.08)	−0.43, −1.15
$Zn(HaaiEt)Cl_2\cdot H_2O$ (**5a**)	37.10(37.24)	3.89(3.95)	15.85(15.80)	420(7.28), 370(18.14), 278(3.62), 230(7.98)	−0.45, −1.22
$Zn(MeaaiEt)Cl_2\cdot H_2O$ (**5b**)	38.99(39.09)	4.32(4.34)	15.21(15.20)	418(6.60), 382(17.64)[s], 370(18.41), 278(4.03), 235(8.52)	−0.49, −1.27
$Zn(ClaaiEt)Cl_2\cdot H_2O$ (**5c**)	33.88(33.94)	3.24(3.34)	14.42(14.40)	438(6.78), 375(19.31), 282(5.19), 245(8.94)	−0.40, −1.12
$Zn(HaaiCH_2Ph)Cl_2\cdot H_2O$ (**6a**)	46.01(46.11)	3.81(3.84)	13.49(13.44)	441(7.41), 377(25.61), 278(4.05), 240(10.46)	−0.47, −1.24
$Zn(MeaaiCH_2Ph)Cl_2\cdot H_2O$ (**6b**)	47.19(47.39)	4.10(4.18)	13.09(13.01)	484(6.67), 384(19.07), 279(3.27), 241(8.15)	−0.50, −1.38
$Zn(ClaaiCH_2Ph)Cl_2\cdot H_2O$ (**6c**)	41.95(42.58)	3.22(3.32)	12.44(12.42)	444(5.38), 380(18.14), 280(4.18) 245(9.88)	−0.42, −1.20
$Zn(HaaiMe)_2(NCS)_2$ (**7a**)	47.61(47.69)	3.57(3.68)	25.23(25.29)	420(3.63), 372(22.34), 338(15.38), 226(8.73)	−0.48, −1.22
$Zn(MeaaiMe)_2(NCS)_2$ (**7b**)	49.48(49.52)	4.09(4.12)	24.00(24.07)	419(2.99), 376(11.03), 338(6.27), 234(4.17)	−0.50, −1.38
$Zn(ClaaiMe)_2(NCS)_2$ (**7c**)	42.35(42.40)	2.83(2.89)	22.43(22.48)	440(7.18), 378(17.62), 360(23.45), 232(8.56)	−0.43, −1.15
$Zn(HaaiEt)_2(NCS)_2$ (**8a**)	49.49(49.52)	4.08(4.12)	24.00(24.07)	419(1.87), 372(12.43), 338(13.16), 230(5.58)	−0.46, −1.23
$Zn(MeaaiEt)_2(NCS)_2$ (**8b**)	51.09(51.18)	4.52(4.59)	22.88(22.96)	420(7.75), 376(28.20), 338(16.16), 236(10.20)	−0.50, −1.28
$Zn(ClaaiEt)_2(NCS)_2$ (**8c**)	44.20(44.27)	3.32(3.38)	21.48(21.52)	436(6.99), 376(17.54), 362(23.68), 228(6.87)	−0.43, −1.14
$Zn(HaaiCH_2Ph)_2(NCS)_2$ (**9a**)	57.79(57.83)	3.91(3.96)	19.78(19.84)	420(8.15), 376(18.71), 338(13.71), 234(8.07)	−0.42, −1.21
$Zn(MeaaiCH_2Ph)_2(NCS)_2$ (**9b**)	58.81(58.89)	4.31(4.36)	19.00(19.08)	418(5.26), 380(17.89), 338(13.71), 234(8.07)	−0.50, −1.39
$Zn(ClaaiCH_2Ph)_2(NCS)_2$ (**9c**)	52.62(52.67)	3.30(3.35)	18.01(18.07)	438(6.99), 376(17.54), 362(23.68), 228(6.87)	−0.45, −1.21

[a] Calculated values are in parenthesis.
[b] Solvent: $CHCl_3$.
[c] Solvent: CH_3CN, electrodes: Pt-disk (working), Pt-wire (auxiliary), SCE (reference), supporting electrolyte [n-Bu_4N][ClO_4], scan rate, 50 mV s^{-1}, solute concentration $\sim 10^{-3}$ M, E_{PC} (cathodic peak potential) in V.

idealized, calculated positions while water hydrogen atoms were located in the difference Fourier maps and subsequently refined according to the riding model. Data reduction, structure solution and refinement were performed with SHELX-97,

3. Results and discussion

3.1. Synthesis and formulation

1-Alkyl-2-(arylazo)imidazoles (RaaiR′, **1**–**3**) are a N,N'-bidentate donor system. The donor centers are abbreviated as N (3) (imidazole) as N and N(azo) as N'. From a methanolic solution of $ZnCl_2$ and RaaiR′ in 1:1 mole proportion we have isolated an orange–yellow crystalline product of composition $Zn(RaaiR')Cl_2\cdot H_2O$ (**4**–**6**). Even in the presence of an excess amount of ligand (> 3 mol) under refluxing conditions the complex of this composition is inserted. The reaction of $ZnCl_2$ with RaaiR′ in the presence of NH_4CNS however has synthesized $Zn(RaaiR')_2(NCS)_2$ (**7**–**9**). Use of $Zn(NO_3)_2$ instead of $ZnCl_2$ has also isolated $Zn(RaaiR')_2$ $(NCS)_2$ (**7**–**9**).

Thermogravimetric studies of $Zn(RaaiR')Cl_2\cdot H_2O$ show water losses at 403–410 K followed by the ligand elimination at 515–525 K. This observation accounts for the coordinated water in a hydrogen bonded network. $Zn(RaaiR')_2(NCS)_2$ on heating explodes at > 675 K and was not studied further. Microanalytical data and zinc analysis (complexometrically) [17] support the composition of the complex and for one case of each type of complex the structures are established by a single-crystal X-ray diffraction study.

3.2. Molecular structure and 1D polymer of $Zn(MeaaiMe)Cl_2\cdot H_2O$ (**4b**)

The crystal structure of $Zn(MeaaiMe)Cl_2\cdot H_2O$ (**4b**) is shown in Fig. 1 and bond parameters are listed in Table

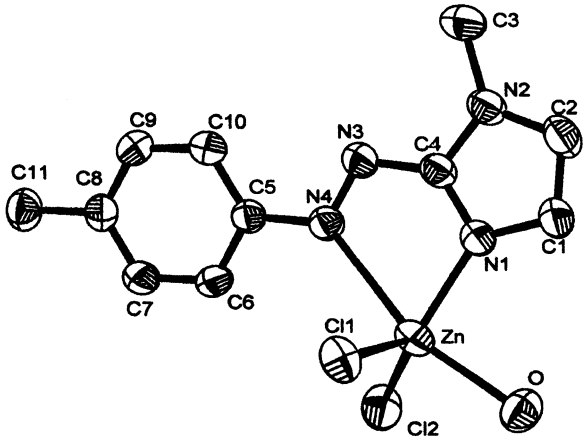

Fig. 1. X-ray structure of $Zn(MeaaiMe)Cl_2\cdot OH_2$ (**4b**).

Table 3
Selected bond lengths (Å) and angles (°) of $Zn(MeaaiMe)Cl_2 \cdot H_2O$ (**4b**) with esd

Bond lengths		Angles	
Zn–N(1)	2.017(2)	N(1)–Zn–O	92.15(9)
Zn–O	2.159(2)	N(1)–Zn–Cl(1)	108.31(7)
Zn–Cl(2)	2.223(1)	N(1)–Zn–Cl(2)	134.07(7)
Zn–Cl(1)	2.256(1)	Cl(1)–Zn–Cl(2)	116.00(4)
N(1)–C(4)	1.325(3)	Cl(1)–Zn–O	100.84(7)
N(1)–C(1)	1.372 (3)	Cl–Zn–O	91.01(7)
N(3)–N(4)	1.269(3)	N(4)–Zn–N(1)	70.6(4)
Zn–N(4)	2.546(3)	N(4)–Zn–Cl(1)	90.5(6)
		N(4)–Zn–Cl(2)	96.9(7)
		N(4)–Zn–O	161.8(7)

Selected bond lengths (Å) and angles (°) of $[Zn(HaaiMe)_2(NCS)_2$ (**7a**) with esd

Bond lengths		Angles	
Zn–N(1)	1.943(3)	N(1)–Zn–N(2)	110.05(12)
Zn–N(2)	1.987(3)	N(1)–Zn–N(3)	83.2(8)
Zn–N(3)	2.726(1)	N(1)–Zn–N(5)	126.98(12)
Zn–N(5)	1.995(3)	N(1)–Zn–N(9)	102.74(11)
Zn–N(7)	2.976(2)	N(2)–Zn–N(3)	86.7(2)
Zn–N(9)	2.079(3)	N(2)–Zn–N(5)	110.72(11)
N(3)–N(4)	1.262(4)	N(2)–Zn–N(9)	95.91(11)
N(7)–N(8)	1.258(4)	N(3)–Zn–N(5)	66.86(5)
		N(3)–Zn–N(9)	172.1(1)
		N(5)–Zn–N(9)	105.23(10)
		C(13)–N(7)–N(8)	114.4(3)
		C(19)–N(9)–Zn	127.9(2)

3. The structure shows a distorted trigonal bipyramidal (TBP) geometry around Zn(II). The coordination includes the chelated azoimine Zn–(N=C–N=N–) group, two Zn–Cl bonds and one $Zn–OH_2$ bond. The atomic arrangements Zn, Cl (1), Cl (2), N(1) constitute a trigonal plane and Zn is deviated by 0.16 Å from the mean plane. The chelate angle is 70.6(4) Å and is the shortest so far reported [10,11] in the series of chelated arylazoimidazole complexes. This may be the reason for the distortion from the symmetric TBP geometry. The N(4), [*N*(azo)] and coordinated OH_2 appear as the apices to the trigonal plane. The Zn–N(4) [Zn–N(azo)] is the longest (2.546(3) Å) one in the family of M–N(azo) bond lengths so far know in the literature [10,11]. The elongation may be due to axial coordination of N(4) with reference to the trigonal plane described by $ZnNCl_2$ and from the small chelate bite angle. 1-Methyl-2-(*p*-tolylazo)imidazole is planar and N(2) (*N*-Methyl) suffers maximum deviation to downward by −0.106 Å. Imidazole and *p*-tolyl rings are joined by an azo group and the dihedral angle is 7.81°. The N = N bond length is 1.269(3) Å and is slightly elongated compared to that of the free ligand value (1.250(1) Å) [18–20]. The stability of the chelated azoimine M–(N=C–N=N–) is due to the metal-to-ligand π-back bonding and the azo group is directly involved in this process [10,11]. This reduces the M–N(azo) bond length and subsequently increases the N=N bond length from that of the free ligand values [10,11,21–23]. Zn(II) is not a sufficiently good π back donor to affect the N = N bond length. The acute chelate angle may develop a strain that is relieved partially by structural distortion and bond length elongation.

The molecular packing shows a 1D polymer running along the a-axis (Fig. 2). The network is constituted via hydrogen bonding of two rows of $Zn(N,N')Cl_2 \cdot OH_2$ in an interlocking fashion [24]. The coordinated H_2O of one molecule in a row interacts via hydrogen bonding with two adjacent molecules [(Zn′)Cl′···H(O)H···Cl′(Zn′)···] of the second row nd vice-versa. This constitutes an eight-member chair-type bi-hydrogen bonded ring and propagates via edge-sharing of Zn–O bonds. The angle extended by the hydrogen bonding three atom system (O–H···Cl) are ∼166° where Cl is coming from the neighbouring atom. Sequence of H-bond parameters: D–H···A, distances of D–H, H–A and D···A, (Å) and angles D–H···A, (°) are as given: O–H(1A), 0.7426; H(1A)···Cl(2), 2.4241; O–Cl(2), 3.1486; O–H(2B)), 0.8023; H(2B)···Cl(1), 2.3684; O–Cl(1), 3.1578; O–H(1A)–Cl(2), 165.54; O–H(2B)···Cl(1), 167.85.

3.3. Molecular structure of $Zn(HaaiMe)_2(NCS)_2$ (**7a**)

The molecular structure of $Zn(HaaiMe)_2(NCS)_2$ (**7a**) is shown in Fig. 3 and bond parameters are given in

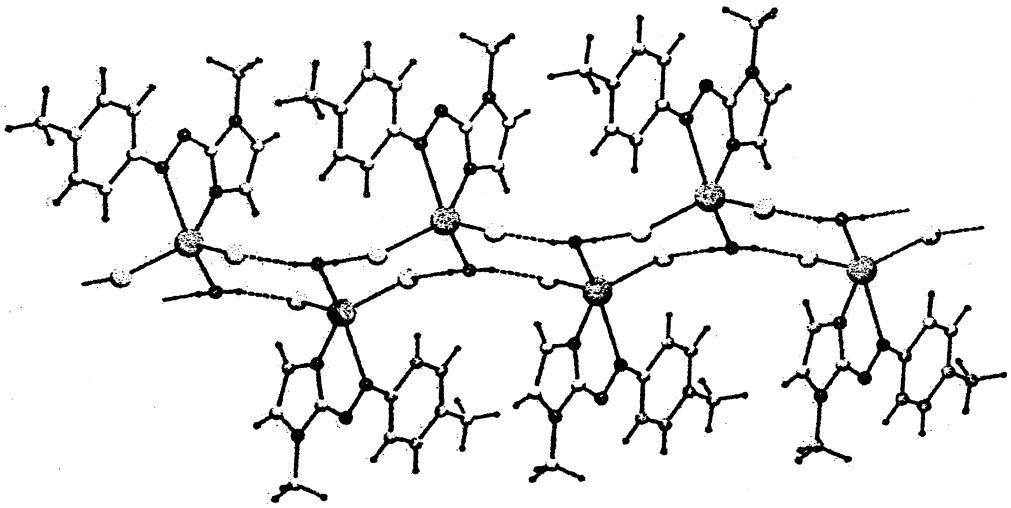

Fig. 2. Hydrogen bonded 1D chain of **4b**.

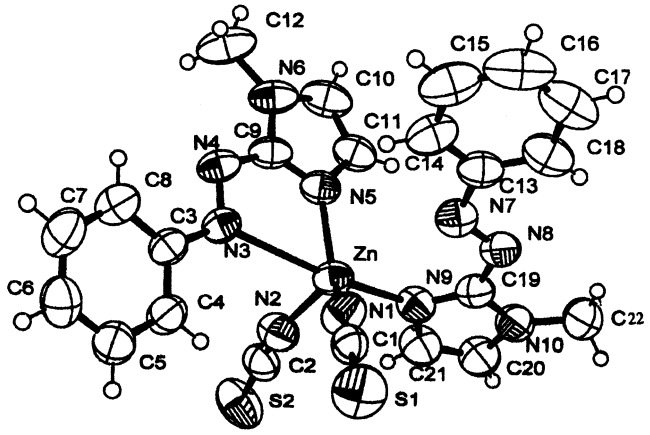

Fig. 3. X-ray structure of $Zn(HaaiMe)_2(NCS)_2$ (**7a**).

Table 3. The structure shows distorted TBP symmetry around Zn(II). This is a rare example where one HaaiMe binds as a *N*,*N*′-chelator and the second molecule acts as a monodentate N-donor ligand. The coordination sphere ZnN_5 is coming from a *N*,*N*′-chelator (one of the HaaiMe ligands forms a chelate ring and is abbreviated as ligand (i)) and *N*(imidazole) (from the second HaaiMe molecule which is abbreviated as ligand (ii)) and two N-centers from the NCS groups. The trigonal plane, ZnN_3 is constituted of two NCS groups and *N*(imidazole) of ligand (i). Two axial positions are occupied by N(3) (N(azo) of ligand (i)) and N(9))*N*(imidazole) of ligand (ii)). The structural distortion of the complex is reflected from the inequivalence of all five Zn–N bond distances and bond angles; even the two Zn–NCS bond lengths are different (Zn–N(1)CS, 1.943(3); Zn–N(2)CS, 1.987(3) Å). This distortion may be due to the small chelate bite angle, N(5)–Zn–N(3), 66.8(6)° which allows closer approach of Zn–N(5) to Zn–N(2). Thus the N(5)–Zn–N(2) angle (110.7(2)°) is less than that of N(5)–Zn–N(1), 126.9(8)°. The Zn–N(3) bond distance (2.72(6) Å) is will below the sum of the van der Waals radii (2.96 Å) of the members [25] while the estimated Zn–N(7) length (2.97(6) Å) is greater than 2.96 Å. Thus ligand (ii) behaves as a monodentate N-donor system. Because of the higher affinity of imidazole-N to Zn(II) out of *N*(imidazole) and *N*(azo) in the ligand, the Zn(II) prefers to bind *N*(imidazole). This is also supported from the structures of zinc-metalloenzymes/proteins [2,3]. The trans angle N(3)–Zn–N(9) is 172.1(1)° and is in accordance with the structural distortion. This is again supported by the N=N bond distance data: N(3)–N(4), 1.262(4) Å is longer than N(7)–N(8), 1.258(9) Å. The later bond length (N(7)–N(8)) is closer to the free ligand values [18–20]. The azophenyl group is freely suspended from the imidazole back bone and makes a dihedral angled 10.90° in the chelated ligand (i). The monodentate ligand (ii) is more planar than ligand (i) and the pendant phenyl group makes a dihedral angle of the 3.8° with the imidazole ring.

3.4. Spectral studies

The infrared spectra of **4**–**6** show a broad medium intense band centered at 3400–3500 cm^{-1} and is assigned to $\nu(H_2O)$. The N=N and C=N vibrations are observed at 1380–1390 cm^{-1}, respectively. The (Zn–Cl) vibrations appear at 315–355 and 280–300 cm^{-1}. On exposure to hotair at 425 K in an oven the complexes turned brown and do not exhibit the broad stretch corresponding to $\nu(H_2O)$. In complexes **7**–**9** a high intense stretch at 2090 $cm^{-1}$is assigned to ν (NCS).

UV–Vis spectra of the complexes in chloroform solution exhibit intense transitions around 280 and 380 nm along with a weak transition at 415–450 nm. On comparing with the free ligand spectra [9] we may conclude that the first two transitions refer to intramolecular charge transfer transitions ($n \rightarrow \pi^*$ and $\pi \rightarrow \pi^*$) and the third transition may be assigned to charge

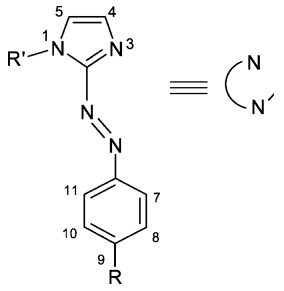

Scheme 1. R′ = Me (**1/4/7**), CH_2CH_3 (**2/5/8**), CH_2Ph (**3/6/9**); R = H (a), CH_3 (b), Cl (c).

transfer between zinc(II) and the ligand [14]. The spectral data are collected in Table 2.

The ^1H NMR spectra of the complexes were collected in CD_3CN and were compared with the free ligand values [9] to determine the binding mode of the complexes. The proton numbering scheme is shown in Scheme 1. The assignment has been made on the basis of spin–spin interaction and changes therein on substitution [9,21] (Table 4). The lower frequency resonances (< 7.5 ppm) suffer significant perturbation on substitution (R) and have been referred to aryl-H (7-H–11-H) signals. The protons, 8,10-H have been particular perturbed by the substituent, 9-R, because of the direct influence of R at the C–H group in the *ortho* position. Imidazolic protons (4- and 5-H) appear at a higher frequency position, > 8 ppm and have been downfield shifted by > 1.00 ppm compared to the free ligand values [9]. This supports the zincophilicity of imidazole-N, which is a normal feature in zinc-metalloenzymes [26]. Zinc(II)-arylazopyrimidine complexes ($Zn(aapm)Cl_2 \cdot CH_3OH$) also exhibit a similar proton signal pattern [14]. The most significant feature is the difference in frequency ($\Delta\delta$) of heterocyclic protons from that of free ligand values; the 4 and 5-H for imidazole in $Zn(RaaiR')Cl_2$ and 4,5, and 6-H for pyrimidine in $Zn(aapm)Cl_2$. The present series of complexes exhibit higher $\Delta\delta > 1.00$ ppm than that of $Zn(aapm)Cl_2 \cdot CH_3OH$ ($\Delta\delta = 0.1–0.8$ ppm) although pyrimidine is more π-acidic than imidazole [26].This supports stronger interaction between Zn(II)-imidazole than that of Zn(II)-pyrimidine. Imidazole being a weaker π-acidic heterocycle interacts strongly with borderline class of metal ion, zinc(II), than that of pyrimidine. In the complexes $[Zn(RaaiR')_2(NCS)_2]$ (**7–9**) imidazole protons,(4-H and 5-H) shift to a more downfield position compared to $Zn(RaaiR')Cl_2$ (**4–6**). It may be due to the combined effect of a more electron withdrawing –NCS compared to –Cl and strong Zn–N(imidazole) bonding. Aryl protons (7H–11H) remain almost unperturbed compared to the free ligand values.

3.5. Electrochemistry

Arylazoimidazoles are non-innocent molecules. They exhibit quasireversible to irreversible azo reductions $(-N{=}N-)/(-N{=}N-)^-$ and $(-N^{\cdot\cdot\cdot}N-)^-/(-N{-}N-)^{2-}$.

Table 4
^1H NMR spectral data [a] of zinc(II) complexes (**4–9**) at 300 K

Compound	δ (ppm) (J (Hz))								
	4-H [b]	5-H [b]	7, 11-H [b]	8,10-H [b]	9-R	1-CH_3 [e]	1-CH_2	(1-CH_2)CH_3	Ph-H
4a	8.13 (7.5)	8.10 (7.8)	7.65 (8.1)	7.50 [c]	7.50 [d]	4.06			
4b	8.07 (7.5)	8.05 (7.8)	7.53 (8.1)	7.33 (6.0)	2.45 [f]	4.04			
4c	8.15 (7.2)	8.10 (7.5)	7.70 (7.8)	7.57 (6.4)		4.10			
5a	8.18 (7.5)	8.11 (7.5)	7.70 (7.8)	7.53 [c]	7.53 [d]		4.63 [g]	1.59[h] (6.0)	
5b	8.09 (7.2)	8.06 (7.5)	7.61 (8.1)	7.36 (6.0)	2.45 [f]		4.52 [g] (8.0)	1.53[h] (6.0)	
5c	8.21 (7.2)	8.13 (7.8)	7.74 (8.1)	7.60 (6.4)			4.63 [g] (11.0)	1.58[h] (6.0)	
6a	8.14 (7.5)	8.11 (7.5)	7.69 (7.8)	7.49 [c]	7.49 [d]		5.53 [e]		7.30–7.40
6b	8.16 (7.5)	8.14 (7.8)	7.65 (7.8	7.37 (6.4)	2.47 [f]		5.62 [e]		7.30–7.45
6c	8.20 (7.5)	8.14 (7.5)	7.69 (7.8)	7.52 (6.0)			5.65 [e]		7.35–7.45
7a	8.30 (7.0)	8.24 (7.5)	7.60 (8.1)	7.50 [c]	7.50 [d]	4.11			
7b	8.20 (7.5)	8.16 (8.0)	7.52 (7.8)	7.35 (7.2)	2.42 [f]	4.10			
7c	8.36 (7.5)	8.26 (8.0)	7.66 (8.1)	7.55 (6.4)		4.15			
8a	8.36 (7.0)	8.25 (8.0)	7.65 (8.1)	7.50 [c]	7.48 [d]		4.70 [g]	1.58[h] (7.5)	
8b	8.27 (7.5)	8.21 (7.8)	7.56 (8.1)	7.32 (6.9)	2.40 [c]		4.58 [g]	1.55 (7.5)	
8c	8.42 (7.5)	8.34 (8.1)	7.69 (8.1)	7.55 (6.9)			4.68 [g]	1.55[h] (6.0)	
9a	8.35 (7.8)	8.25 (8.1)	7.61 (8.1)	7.45 [c]	7.45 [d]		5.60 [e]		7.30–7.40
9b	8.32 (7.5)	8.22 (7.8)	7.58 (7.8)	7.33 (7.2)	2.42 [f]		5.65 [e]		7.30–7.40
9c	8.48 (7.8)	8.39 (7.8)	7.63 (7.8)	7.47 (7.2)			5.70 [e]		7.30–7.45

[a] Solvent: CD_3CN.
[b] Doublet.
[c] Multiplet.
[d] δ(9-H).
[e] Singlet.
[f] δ(9-Me).
[g] Quartet.

Zinc(II) is electroinactive in the potential range 1.5 to −1.5 V versus SCE. The complexes exhibit two/three irreversible cyclic voltammetric responses in the potential range 0.0 to −1.5 V versus SCE (Table 2). Voltammetric waves exhibit cathodic response (E_{PC}, cathodic peak potential, V) and on scan reversal anodic peaks are rarely obtained. This accounts instability of the reduced species. On comparing with the voltammogram of the free ligand, these responses may correspond to azo reductions [9,21]. The shifting of potential data to a more positive value in the complexes than the free ligand may be due to electron drifting by the metal ion on coordination to the ligand.

3.6. EHMO calculation

Crystallographic data of $Zn(MeaaiMe)Cl_2 \cdot H_2O$ and $[Zn(HaaiMe)_2(NCS)_2$ were used as a model for extended Huckel calculation to find out the approximate composition of the frontier orbitals.It is observed that both the HOMO and LUMO are constituted by ligand orbitals. The HOMO is 89% and the LUMO is 86% ligand orbitals. The HOMO contains 62% imidazole and 27% arylazo functions. The LUMO is made up of 75% azo orbitals. Thus, the spectral transitions in the UV–Vis region are intramolecular ($n \rightarrow \pi$, $\pi \rightarrow \pi^*$) charge-transfer transition. The oxidation is regarded as an electron extraction from the HOMO and the reduction is referred to as electron accommodation at the LUMO. The complexes exhibit only reduction. We conclude that reduction of the azo function is taking place.

4. Supplementary material

Crystallographic data for the structural analysis has been deposited with the Cambridge Crystallographic Data Centre, CCDC No. 186346 for $Zn(MeaaiMe)Cl_2 \cdot H_2O$ and CCDC No. 184362 for $[Zn(HaaiMe)_2(NCS)_2$. Copies of this information may be obtained free of charge from the Director, CCDC, 12 Union Road, Cambridge, CB2 1EZ, UK. (fax: +44-1223-336033; e-mail: deposit@ccdc.cam.ac.uk or www: http://www.ccdc.cam.ac.uk).

Acknowledgements

Financial support from the University Grants Commission New Delhi is gratefully acknowledged. We thank professor N. Roychowdhury, IACS, Kolkatta for thermal studies. Our sincere thanks are due to Dr Babu Vargheese, Regional Sophisticated Instrumentation Center, IIT, Madras and Dr Golam Mostafa, Department of Physics, National Tsing Hua University, Hsinchu 300, Taiwan, ROC for his help in solving the X-ray structures.

References

[1] H. Eklund, C.-I. Branden, in: T.G. Spiro (Ed.), Zinc Enzymes, Wiley, New York, 1983, p. 124.
[2] W. Kaim, B. Schwederski, Bioinorganic Chemistry: Inorganic Elements in the Chemistry of Life, Wiley, New York, 1994.
[3] R.G. Matthews, Acc. Chem. Res. 34 (2000) 618 (and references therein).
[4] S. Nagasato, Y. Sunatsuki, S. Ohsato, T. Kido, N. Matsumoto, M. Kojima, Chem. Commun. 2 (2002) 14.
[5] C. Plaee, J.-L. Zimmermann, E. Mulliez, G. Guillot, C. Bois, J.-C. Chottard, Inorg. Chem. 37 (1998) 4030.
[6] H. Hayashi, M. Goto, M. Shionoya, E. Kinrura, Inorg. Chem. Commun. 3 (2000) 107.
[7] Z.-W. Mao, G. Liehr, R. Van Eldik, J. Chem. Soc., Dalton Trans. (2001) 1593.
[8] E. Kimura, Acc. Chem. Res. 34 (2001) 171.
[9] T.K. Misra, D. Das, C. Sinha, Polyhedron 16 (1997) 4163.
[10] S. Pal, D. Das, C. Sinha, C.H.L. Kennard, Inorg. Chim. Acta 21 (2001) 313.
[11] P. Byabartta, S. Pal, T.K. Misra, C. Sinha, F.-L. Liao, K. Panneerselvam, T.-H. Lu, J. Coord. Chem. 55 (2002) 479 (and references therein).
[12] D. Das, A.K. Das, C. Sinha, Talanta. 48 (1999) 1013.
[13] B.C. Mondal, D. Das, A.K. Das, J. Indian Chem. Soc. 78 (2001) 89.
[14] J.K. Nag, P.K. Santra, C. Sinha, F.-L. Liao, T.-H. Lu, Polyhedron 20 (2001) 2253.
[15] K. Bag, T.K. Misra, C. Sinha, J. Indian Chem. Soc. 75 (1998) 421.
[16] K. Bag, N.K. De, B.R. De, C. Sinha, Proc. Indian Acad. Sci. (Chem. Sci.) 109 (1997) 159.
[17] A.I. Vogel, A Text-Book of Quantitative Inorganic Analysis, 3rd ed., ELBS, Longman, 1975, p. 433.
[18] D. Das, Ph.D. thesis, 1998, Burdwan University, Burdwan.
[19] A. Saha, C. Das, S. Goswami, S.-M. Peng, Indian J. Chem. 40A (2001) 198.
[20] H.-K. Fun, K. Chinnakali, H.-F. Chen, X.-H. Zhu, X.-Z. You, Acta Cryst. 25 (1999) 99.
[21] T.K. Misra, D. Das, C. Sinha, P.K. Ghosh, C.K. Pal, Inorg. Chem. 37 (1998) 1672.
[22] G.K. Routh, S. Pal, D. Das, C. Sinha, A.M.Z. Slawin, J.D. Woollins, Polyhedron 20 (2001) 363.
[23] P. Byabartta, J. Dinda, P.K. Santra, C. Sinha, K. Panneerselvam, F.-L. Liao, T.-H. Lu, J. Chem. Soc., Dalton Trans. (2001) 2825.
[24] X.-Z. Li, Y. Yu, S.-F. Si, D.-Z. Liao, Z.-H. Jiang, S.-P. Yan, Inorg. Chem. Commun. 5 (2002) 478.
[25] A.G. Orpen, L. Brammar, F.H. Allen, O. Kennard, D.G. Watson, R. Taylor, J. Chem. Soc., Dalton Trans. (1989) SI.
[26] E.C. Constable, Coord. Chem. Rev. 93 (1989) 205.